Proceedings of ICAD2006
4th International Conference on Axiomatic Design
Firenze – June 13-16, 2006
ICAD-2006-43

FE ANALYSES OF STABILITY OF SINGLE AND DOUBLE CORRUGATED BOARDS

Enrico Armentani
enrico.armentani@unina.it
University of Naples
P.le V. Tecchio, 80
80125 Naples
Italy

Francesco Caputo
francesco.caputo@unina2.it
Second University of Naples
Via Roma, 29
81031 Aversa (CE)
Italy

Renato Esposito
renato.esposito@unina.it
University of Naples
P.le V. Tecchio, 80
80125 Naples
Italy

ABSTRACT

This work describes nonlinear finite element analysis of single and double corrugated boards subjected to compressive loading. Detailed modelling of the panels, where liners and flutings are represented, is compared to simplified shell modelling with a solid core. Each layer is modelled as orthotropic and homogenous while material properties are estimated from the in-plane properties of the paper sheet. The solid core stiffness in the model is determined as effective stiffness, equivalent to that of the corrugated medium. Different combinations of stiffness and thickness ratios for the top and bottom layers are examined. The panel is considered to be as simply supported edges. In order to model particular boundary conditions some constraint equations were established for the boundary edges subjected to the loads. In the analysis, both local and global stability have been considered The results from finite element analyses are compared with those from an experimental study. It is shown that a good agreement between the load-displacement paths of numerical analyses and the experimental tests is achieved even when a linear elastic material model is used.

Keywords: Finite Element Analysis, double corrugated board, instability

1 INTRODUCTION

Corrugated board is used mostly as a packaging material, e.g. in storage boxes. It consists of one or several layers of corrugated paper (fluting or core) which is glued between plane sheets of paper (facings or liners). As for a typical sandwich material, the purpose of the facings are to carry normal stresses resulting from in-plane deformation and curvature of the board. The purpose of the core is to carry shear stresses and to keep the facings apart. Since the core is supposed to stabilize the facings it must posses sufficient stiffness against deformation in planes normal to the facings. These two properties give rise to the outstanding strength and stiffness characteristics, compared to the low weight, of a sandwich structure. The distance between the facings also affects the stiffness properties of the sandwich. The larger the distance, the stiffer the composite will be in bending. The layers can be very weak when separated, but together joined they create a stiff composite.

The most important loading case for this type of application is compressive loading, e.g. from boxes standing on top of each other. If a board is overloaded, it will collapse either by structural or by material failure.

Several studies have been published on single corrugated boards. Some authors have determined material elastic properties of corrugated board [1-3]. Nordstrand and Carlsson [4] have shown that the core of a corrugated board has low shear stiffnesses, especially in direction perpendicular to the corrugations, but which are influenced by the manufacturing process [5]. Several authors have investigated the buckling and post-buckling behaviour of corrugated boards [5-9] and corrugated paper packages [10]. Some others have investigated on equivalent stiffness properties of corrugated board in order to obtain a simplified finite element model [5, 11, 12]. Not so much papers have been written on double corrugated boards. Isaksson and Hägglund have investigated the delamination of double corrugated boards subjected to shear and bending loads [13].

In this work detailed finite element analyses (FEA) of single and double corrugated board panels when loaded in-plane are performed. In the detailed analysis, the veritable geometry is modelled, i.e. the liners and the flutings are represented by their actual plane and corrugated geometry. The results from the FEA are compared with those from an experimental study [7]. In addition to the detailed models, simplified models are analysed, where the corrugated layers are replaced by solid cores. The solid core stiffness properties in these models are determined as effective stiffnesses, equivalent to those of the corrugated medium.

2 FINITE ELEMENT MODELS

All considered models are squared panels of 400 mm width, such as those tested in [7]. Because of the double symmetry (Figure 1), just a quarter of panel is modelled, in order to reduce computational efforts. In this way, in the buckling analysis, not symmetric deformed shapes are prevent. Just one analysis on a

full model in buckling and post-buckling behaviour has been performed in order to verify the hypothesis correctness. No differences between symmetric and full models were found, so that the symmetric conditions have been applied for all the others analyses.
FEA have been performed in large displacement condition.

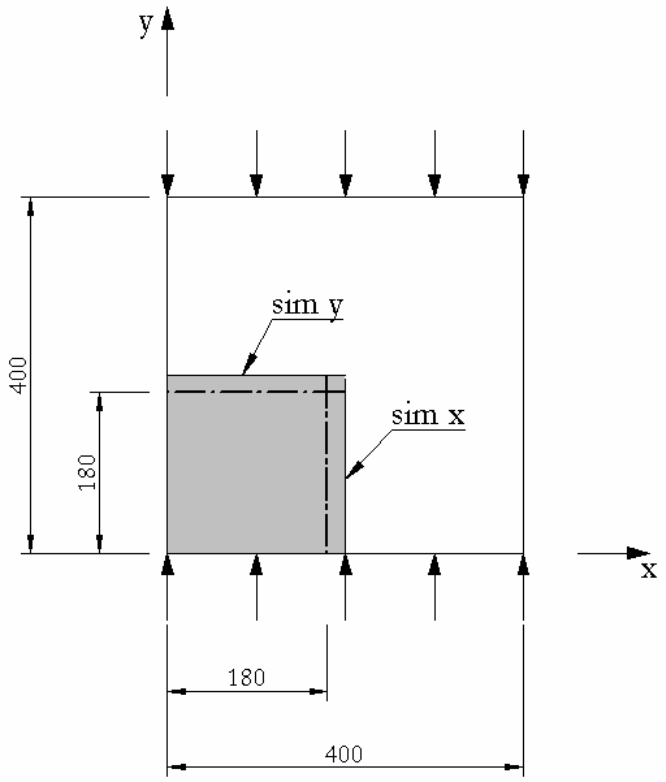

Figure 1 – Studied quarter panel.

2.1 SINGLE CORRUGATED BOARD

Figure 2 shows the transversal dimensions of the single corrugated board, whereas the finite element mesh of detailed model for single corrugated board is shown in Figure 3. Paperboard sheets are modelled with 78,156 isoparametric four-node shell elements and 70,224 nodes.

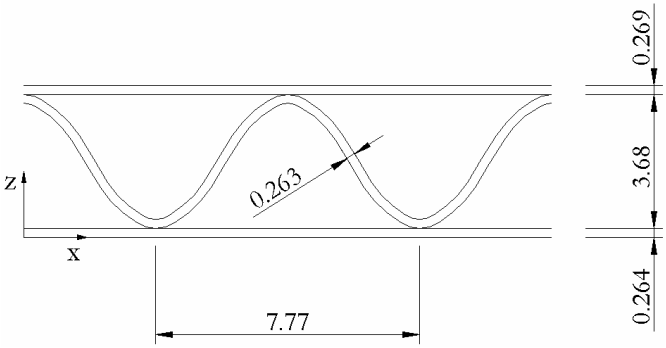

Figure 2 – Dimensions of the single corrugated board, [mm].

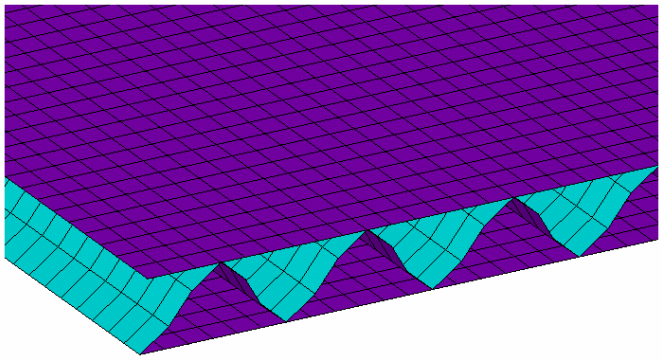

Figure 3 – Finite element mesh of detailed model for single corrugated board.

In order to verify if a simplified composite model provides satisfying results regarding to load-deformation path, a composite model with a solid core was created. Figures 4 and 5 show the detailed model and the simplified model respectively for single corrugated board. The mesh of simplified model is plane and consists of 400 eight-node layered shell elements and 1,281 nodes.

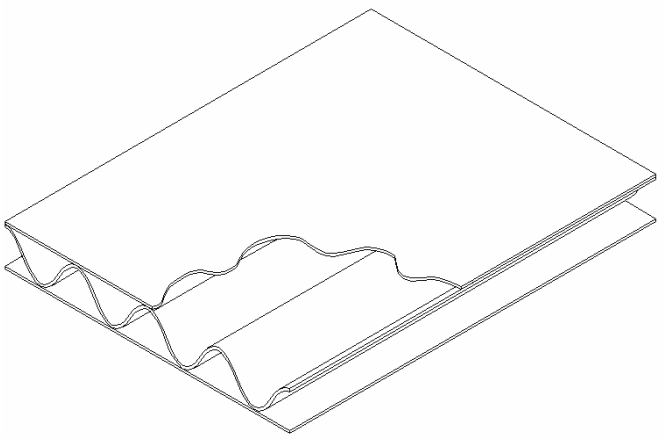

Figure 4 – Detailed model of single corrugated board.

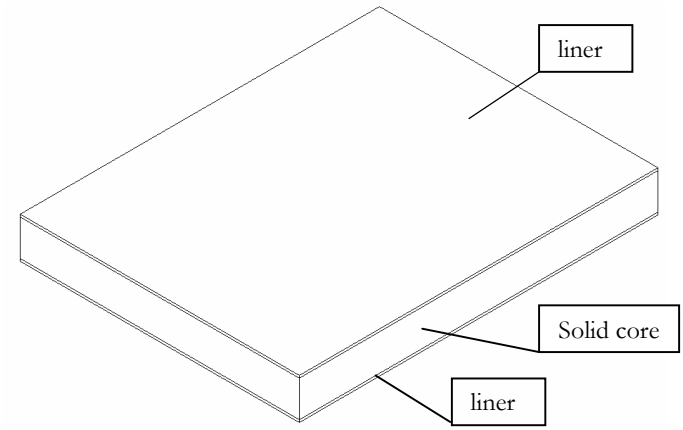

Figure 5 – Simplified model of single corrugated board.

2.2 DOUBLE CORRUGATED BOARD

Two types of double corrugated board are investigated: the first one (Figure 6) with the two flutings having equal wave widths and lengths (the same of single corrugated board) and another one (Figure 7) with superior fluting having different wave width and length respect to the inferior one. The first case is modelled in order to investigate the influence of phase shift between the flutings, while the second case corresponds to a typical manufactured double corrugated board, whereas the narrower wave is employed to improve the in plane deflection strength.
In the first case, with reference to Figure 6, eight finite element models have been investigated for different values of phase shift: $\varphi = 0, \pi/8, \pi/4, \pi/2, \pi, 5\pi/4, 11\pi/8, 3\pi/2$.

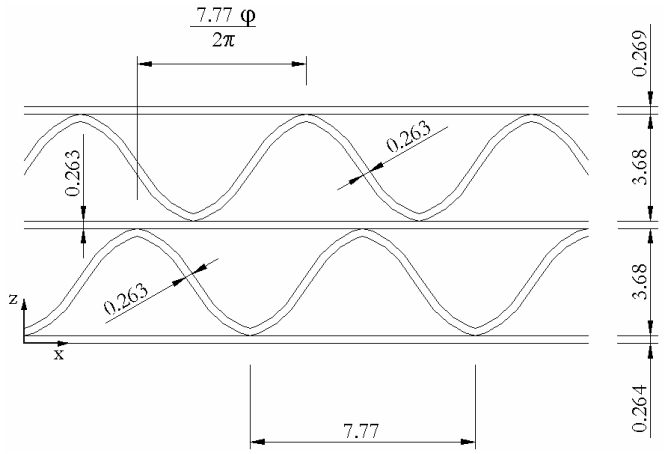

Figure 6 – Dimensions [mm] of the double corrugated board for the first case: equal flutings.

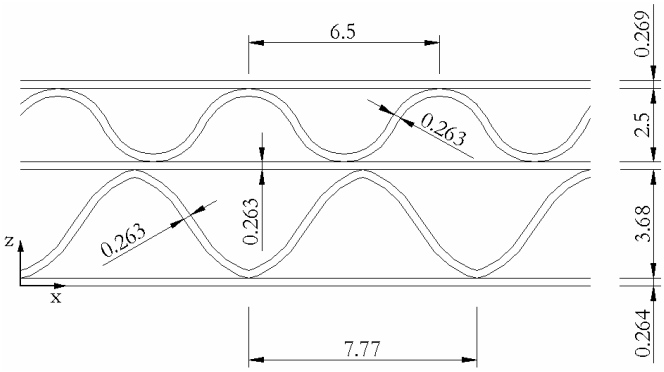

Figure 7 – Dimensions [mm] of the double corrugated board for the second case: different flutings.

For all nine meshes (eight models with equal flutings and one with different flutings), the element number varies from 130,260, for two models with equal flutings and $\varphi = 0$ and π respectively, up to 145,790 for the model with different flutings, whereas the node number varies from 114,072 to 128,017 respectively. Figure 8 refers to equal flutings with $\varphi = \pi/4$, whereas the mesh with different flutings is shown in Figure 9.

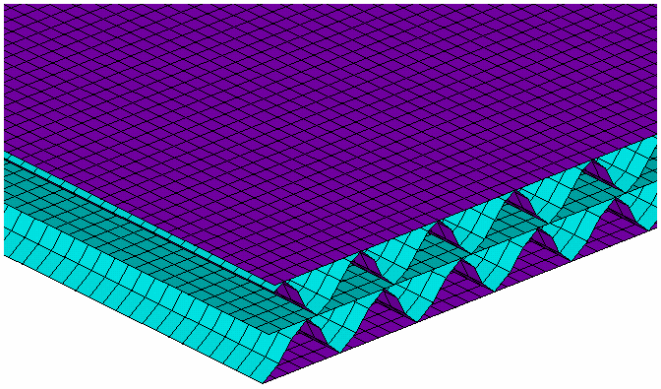

Figure 8 – Finite element mesh of detailed model for double corrugated board with equal flutings ($\varphi = \pi/4$).

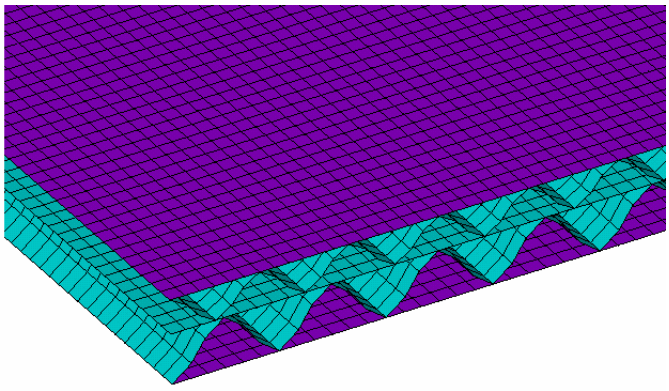

Figure 9 – Finite element mesh of detailed model for double corrugated board with different flutings.

Such as single corrugated board, detailed and simplified models are investigated for double corrugated boards too (see Figures 10 and 11 respectively). Simplified models take in account two solid cores among three liners. The same mesh of the simplified model for single corrugated board, with 400 elements and 1281 nodes, is used.

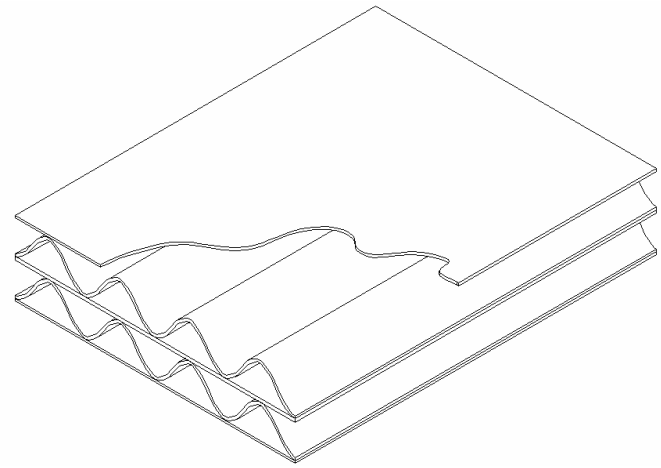

Figure 10 – Detailed model of double corrugated board.

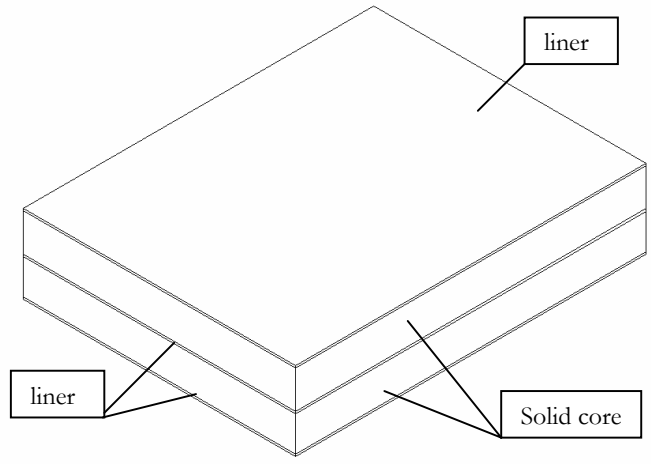

Figure 11 – Simplified model of double corrugated board.

2.3 MATERIALS

The papers are considered as orthotropic and approximated as linear elastic. According to ref. [7] the values reported in Table 1 have been considered.

	Upper liner	Fluting and middle liner	Lower liner	Solid core
Ex [MPa]	7,600	5,400	6,660	5.0
Ey [MPa]	4,020	2,280	3,310	231
Ez [MPa]	38	27	33	3,000
νxy	0.34	0.34	0.34	0.05
νxz	0.01	0.01	0.01	0.01
νyz	0.01	0.01	0.01	0.01
Gxy [MPa]	2,140	1,360	1,820	0.231
Gxz [MPa]	138	98	121	3.5
Gyz [MPa]	115	65	95	35

Tab. 1 – Material properties.

In Table 1 it is assumed, for detailed model, that:

$$Ez = Ex/200 ,$$

according to [3], and

$$Gxy = 0.387\sqrt{ExEy}$$

$$Gxz = Ex/55$$

$$Gyz = Ex/35$$

according to [1, 2].
As above mentioned, a composite model with a solid core was considered for both single and double corrugated boards. Since the fluting has been replaced with a core, the equivalent properties for this layer need to be calculated. The material parameters of the solid core are set according to [7] and they are reported in Table 1.

2.4 BOUNDARY CONDITIONS

In order to simulate correctly the experimental test [7], some constraints have been established for the boundary edges. The panel is considered to be simply supported, i.e. at the free boundary edge (x = 0 mm) the degrees of freedom uz and rotx are set to zero. At symmetry boundary edges (x = 200 mm, y = 200 mm), symmetry conditions are prescribed. At the boundary edge subjected to load (y = 0 mm) some constraint equations are imposed in order to allow rotation about the x-axis and to keep a plane edge during the compression. The translations in the y-direction are described for all nodes by:

$$uy^n + z^n rotx^n - uy^m = 0$$

where n denotes node and m denotes a master node (not involved in the structure) where the load is applied. Note that only degree of freedom uy^m is active for the master node.
The rotations about the x-axis are controlled by the following constraint equations:

$$rotx^u - rotx^f = 0 \text{ and } rotx^f - rotx^l = 0$$

where the upper scripts u, f and l, denote upper liner, fluting and lower liner respectively. The equation imposed for the translation in the z-direction is:

$$uz^u - uz^l = 0$$

3 ANALYSIS AND RESULTS

3.1 SINGLE CORRUGATED BOARD

A preliminary linear buckling analysis has been performed in order to obtain buckling shape and estimate the first critical buckling load (954 N for the detailed model and 1,033 N for the simplified model). Then a geometrically non linear analysis has been performed in order to investigate the post-buckling behaviour. Because of plane mesh, just for simplified model in non linear analysis, an initial out of plane defect of 0.8 mm in the panel central node is imposed in order to induced buckled shape.
Results of these analyses are presented in terms of displacements and load-deformation path.
Figure 12 shows load-out of plane displacement path for numerical models and experimental tests [7] of the panel central node in which there is the maximum displacement. Before buckling phenomena, detailed and simplified models show the same behaviour, but with the initial stiffness higher than those ones of the experimental tests. This is because in the FE analyses, the connections are modelled as a rigid coupling and this makes the stiffness of the structure overestimated. Furthermore, the FE models overestimate the real initial stiffness because they do not take into account real imperfections of the panel. The introduction of local perturbations could also decrease the initial tangential stiffness, so that the load-displacement paths could be in better agreement before large displacements occur. In post-buckling behaviour, simplified model differs from detailed one which shows a better correlation with experimental data.

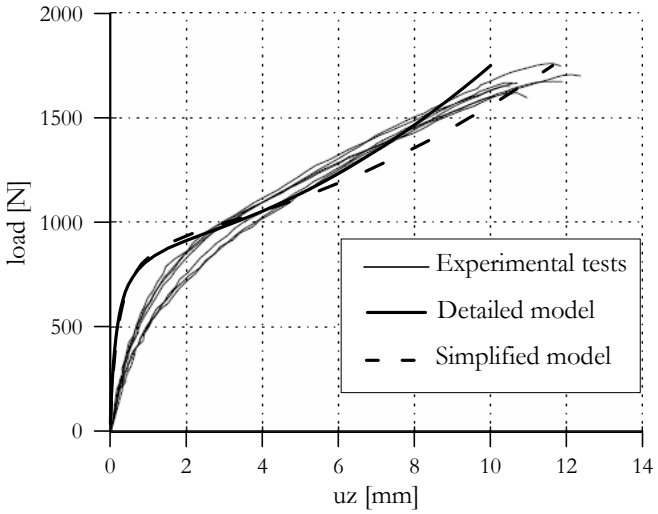

Figure 12 – Load vs. out of plane displacement at point x = y= 200 mm.

In Figure 13 the out of plane displacements of the panel corresponding to load of 1600 N is shown for the simplified model. Similar shape is obtained for the detailed model.

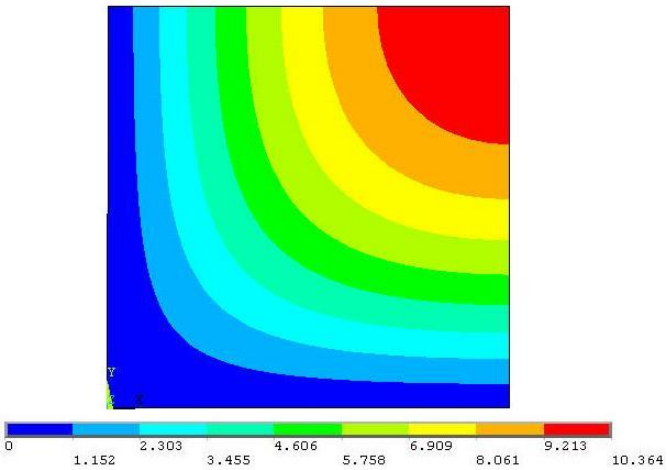

Figure 13 – Global out of plane displacements, uz [mm], for the simplified model (load = 1600 N).

Figures 14 and 15 show a comparison of the section deformed shape at cross sections y = 180 mm and x = 180 mm respectively (see Figure 1) between the FE analyses and the test. They show that both the detailed and the simplified models have section deformed shapes quite similar to the test.

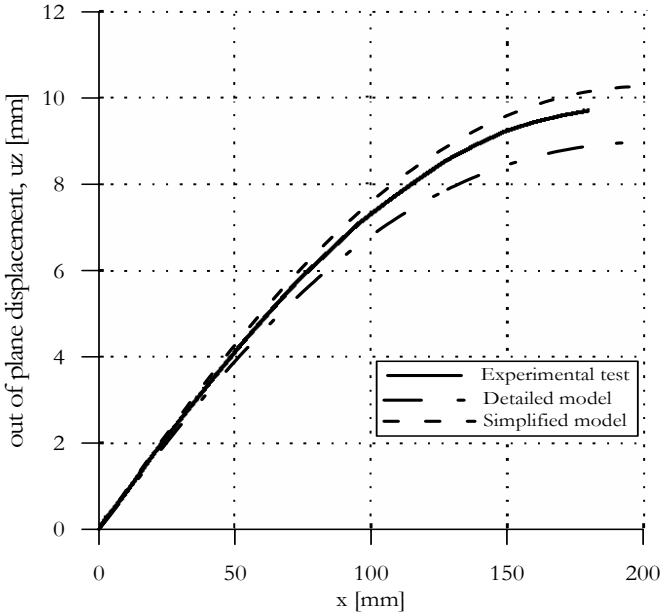

Figure 14 – Global out of plane displacements, uz [mm], at line y = 180 mm (load = 1600 N).

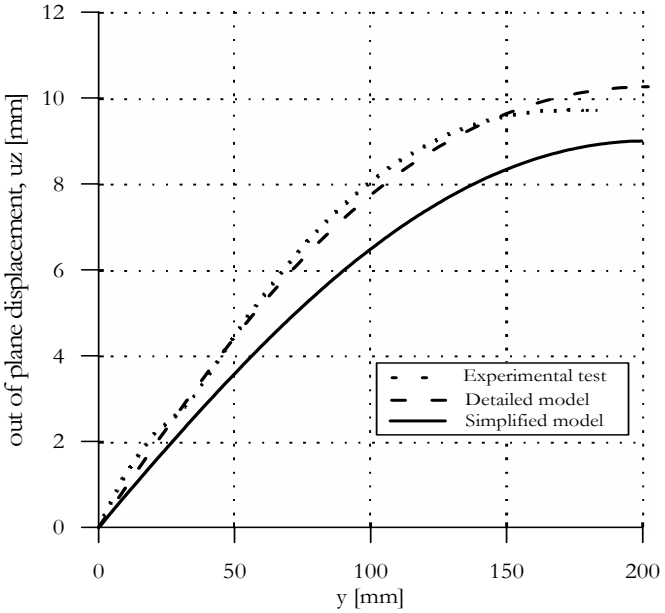

Figure 15 – Global out of plane displacements, uz [mm], at line x = 180 mm (load = 1600 N).

3.2 DOUBLE CORRUGATED BOARD

First critical buckling loads are quite similar for double corrugated boards with equal flutings; they vary from 3,833 N (for $\varphi = \pi$) to 3,956 N (for $\varphi = 0$), while the buckling load drops to 2,876 N for the paper with different flutings.

Figure 16 shows load-out of plane displacement path of the double corrugated boards. Absolute values of out of plane displacements are reported, because of the papers do not show buckled shape on the same side. Results of detailed models are reported. Corrugated boards with phase shift, φ , equal to 0, $\pi/2$, and $5\pi/4$ present the same behaviour, with initial stiffnesses higher than those with $\varphi = \pi/4$, $11\pi/8$ and $3\pi/2$, that are equal to each other. The highest stiffness correspond to $\varphi = \pi/8$, whereas corrugated board with symmetric flutings ($\varphi = \pi$) shows the lowest one. Corrugated board with different flutings has an initial stiffness comparable to equal flutings ones with phase shift equal to 0, $\pi/2$, and $5\pi/4$ (better than corrugated board with $\varphi = \pi$), but large deflections occur at lower loads.

Figure 17 shows differences between detailed and simplified models, for both equal ($\varphi = 0$) and different flutings boards. Like as single corrugated board, the models show the same behaviour before that buckling occurs and they differ slightly when load increases.

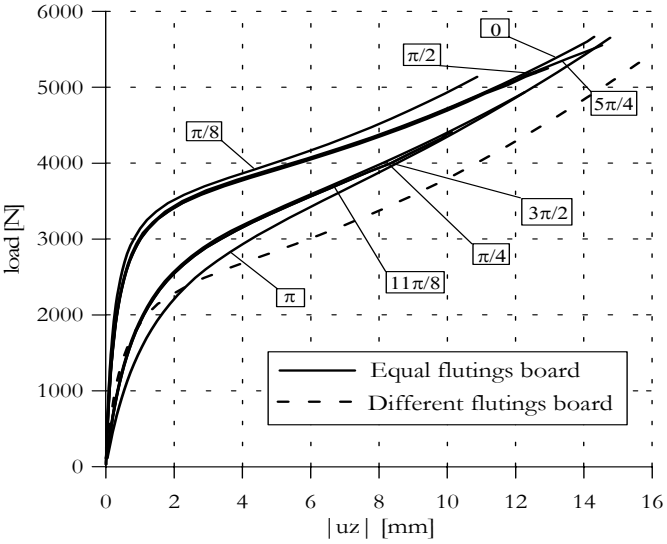

Figure 16 – Load vs. out of plane displacement, at various values of φ, (point x = y= 200 mm).

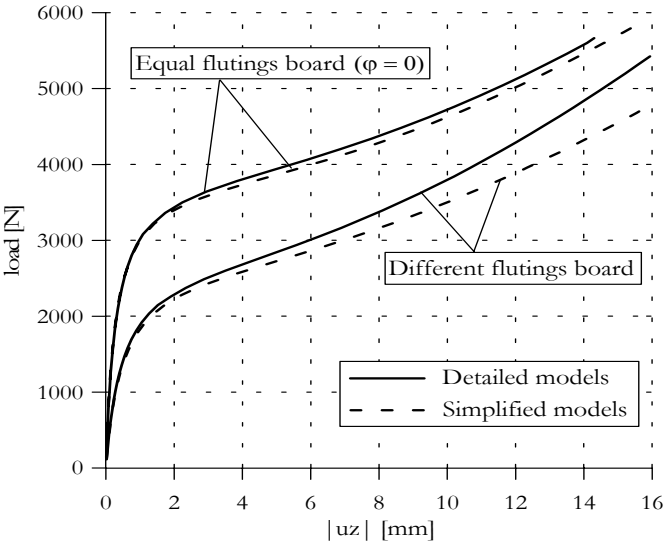

Figure 17 – Load vs. out of plane displacement, for detailed and simplified models.

4 CONCLUSIONS

Some basic remarks can be drawn from this study on corrugated board when subjected to a compressive load.

- The agreement of the load-displacement responses between numerical and experimental results is good even when a linear-elastic material model is used.
- Simplified model gives results very close to detailed model before that buckling phenomenon occurs, for both single and double corrugated boards.
- In post-buckling behaviour simplified model differs from detailed one, but it can be considered acceptable even considering that computational time gets drastically shorter.

5 REFERENCES

[1] R.W. Mann, G.A. Baum, C.C. Habeger, 1980, Determination of all nine orthotropic elastic constants for machine-made paper, *Tappi J.*, 63, 163-166.

[2] G.A. Baum, D.C. Brennan, C.C. Habeger, 1981, Orthotropic elastic constants of paper, *Tappi J.*, 64, 97-101.

[3] K. Persson, 1991, Material Model for Paper: Experimental and Theoretical Aspects, Diploma Report, Lund University, Sweden.

[4] T. Nordstrand, L.A. Carlsson, 1997, Evaluation of transverse shear stiffness of structural core sandwich plates, *Composite Structures*, 37, 145-153.

[5] T. Nordstrand, 1995, Parametric study of the post-buckling strength of structural core sandwich panels, *Composite Structures*, 30, 441-451.

[6] P. Patel, T. Nordstrand, L. A. Carlsson, 1997, Local buckling and collapse of corrugated board under biaxial stress, *Composite Structures*, 39, 93-110.

[7] A. Allansson, B. Svärd, 2001, Stability and collapse of corrugated board, *Structural Mechanics*, Lund University, Sweden.

[8] T. Nordstrand, 2004, Analysis and testing of corrugated board panels into the post-buckling regime, *Composite Structures*, 63, 189-199.

[9] T. Nordstrand, 2004, On buckling loads edge-loaded orthotropic plates including transverse shear, *Composite Structures*, 65, 1-6.

[10] M. E. Biancolini, C. Brutti, Numerical and Experimental Investigation of the Strength of Corrugated Board Packages, 2003, *Packaging Technology and Science*, 16, 47-60.

[11] Z. Aboura, N. Talbi, S. Allaoui, M.L. Benzeggagh, 2004, Elastic behaviour of corrugated cardboard: experiments and modelling, *Composite Structures*, 63, 53-62.

[12] M.E. Biancolini, 2004, Evaluation of equivalent stiffness properties of corrugated board, *Composite Structures*, 69, 322-328.

[13] P. Isaksson, R. Hägglund, 2005, A mechanical model of damage and delamination in corrugated board during folding, *Engineering Fracture Mechanics*, 72, 2299-2315.